

# 1. Introduction

Matter and energy are fundamental components of our physical world. These components manifest themselves in a variety of ways under different physical conditions and can be affected by a variety of processes. Our interest in this first chapter relates specifically to the fusion of light nuclides which forms the basis of energy release in stars and which is expected to be harnessed on earth.

## 1.1 Matter and Energy

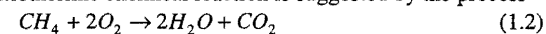
It is a common observation that matter and energy are closely related. For example, a mass of water flowing into the turbines of a hydro-electric plant leads to the generation of electricity; the rearrangement of hydrogen, oxygen, and carbon in chemical compounds in an internal combustion engine generates power to move a car; a neutron-induced splitting of a heavy nucleus produces heat to generate steam; two light nuclei may fuse and immediately break up with the reaction products possessing considerable kinetic energy. Each of these examples illustrates a transformation from one state of matter and energy to another in which an attendant release of energy has occurred.

These matter-energy transformations may be represented in various forms. For the hydro-electric process we may write

$$m(h_1) \rightarrow m(h_2) \quad (1.1)$$

where  $m(h_1)$  and  $m(h_2)$  is a mass of water at an initial elevation  $h_1$  and final elevation  $h_2$ ; the resultant energy  $E$  released can be evaluated by computing  $(mgh_1 - mgh_2)$ , where  $g$  is the local acceleration due to gravity.

An example of an exothermic chemical reaction is suggested by the process



with an energy release of about  $5 \text{ eV}^*$ .

The case of neutron induced fission of a  $^{235}\text{U}$  nucleus is represented by

$$n + {}^{235}\text{U} \rightarrow \nu n + \sum_i P_i \quad (1.3)$$

where  $n$  is a neutron,  $P_i$  is a particular reaction product, and  $\nu$  is the number of neutrons emitted in this particular process. Here, the total energy released possesses a slight dependence on the kinetic energy of the initiating neutron but

---

\* Appendix A provides equivalents of various physical quantities.

is typically close to 200 MeV.

The fusion reaction likely to be harnessed first is given by



with an energy release of 17.6 MeV. Accounting for the fact that the above species react as nuclei, we assign in a more compact notation the names deuteron, triton, and alpha to the reactants and reaction product, to give



The fundamental features of matter and energy transformation are thus evident. In the hydroelectric case, a mass of water has to be raised to a higher level of potential energy—performed by nature's water cycle—and it subsequently attains a lower state with the difference in potential energy appearing as kinetic energy available to generate electricity. For the case of chemical combustion, an initial energetic state of the molecules corresponding to the ignition temperature of the fuel, has to be attained in order to induce a chemical reaction yielding thereupon new chemical compounds. The energy release thereby is due to the more tightly bound reaction product compounds with a slightly reduced total mass; such a mass defect is generally manifested in energy release—typically in the eV range for chemical reactions. In the case of fission, the initiating neutron needs to possess some finite kinetic energy in order to stimulate the rearrangement of nuclear structure; interestingly, the thermal motion of a neutron at room temperature is sufficient for the case involving nuclei such as  ${}^{235}\text{U}$ . For fusion to occur, the reacting nuclei must possess sufficient kinetic energy to overcome the electrostatic repulsion associated with their positive charges before nuclear fusion can take place; the alternative of fusion reactions at low temperature is also possible and will be discussed later. Again, in the case of fission and fusion, the reaction products emerge as more tightly bound nuclei and hence the corresponding mass defect determines the quantity of nuclear energy release—typically in the MeV range.

Evidently then, a more complete statement of the above processes is therefore provided by writing an expression containing both matter and energy terms in the form

$$E_{in} + M_{in} \rightarrow E_{out} + M_{out} \quad (1.6)$$

with the masses measured in energy units, i.e. multiplied by the square of the speed of light. The corresponding process is suggested graphically in Fig.1.1.

The depiction of Fig.1.1 suggests some useful generalizations. Evidently, a measure of the effectiveness and potential viability for energy generation by such transformations involves microscopic and macroscopic details of matter-energy states before and after the process. In addition, it is also necessary to include considerations of the relative supply of the fuel,  $M_{in}$ , the toxicity of reaction products,  $M_{out}$ , the magnitude of  $E_{out}$  relative to  $E_{in}$ , as well as other technological, economic and ecological considerations. Additional issues may include availability of the required technology, deployment schedules, energy conversion losses, management and handling of the fuel and of its reaction products.

economic cost-benefit, environmental impact, and others.



Fig. 1.1: Schematic depiction of matter and energy flow in a matter-energy transformation device. The length of the arrows is to suggest a decrease in mass flow,  $M_{out} < M_{in}$ , with a corresponding increase in energy flow,  $E_{out} > E_{in}$ .

## 1.2 Matter and Energy Accounting

Conservation conditions are fundamental aids in the quantitative assessment of nuclear processes. Of paramount relevance here is the joint conservation of nucleon number and energy associated with an initial ensemble of interacting nuclear species of type a and type b which, upon a binary collisional interaction, yield two particles of type d and e:

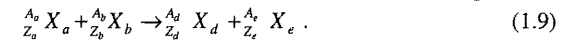


Note that the details of the highly transient intermediate processes are not listed—only the initial reactants and the final reaction products are shown.

An accounting of all participating nucleons is aided by the notation

$${}^A_Z X = \left( \begin{array}{l} \text{nuclear species named X containing} \\ \text{A nucleons of which Z are protons} \end{array} \right) \quad (1.8)$$

and therefore yields the more complete statement for the reaction of Eq.(1.7) in a form which lists the number of nucleons involved in this nuclear rearrangement:



Recall that  $A_j$  is the sum of  $Z_j$  protons and  $N_j$  neutrons in the nucleus,  $A_j = Z_j + N_j$ . Nucleon number conservation therefore requires

$$A_a + A_b = A_d + A_e \quad (1.10)$$

and, similarly for charge conservation we write

$$Z_a + Z_b = Z_d + Z_e. \quad (1.11)$$

Characterization of energy conservation for reaction (1.7) follows from the knowledge that the total energy  $E^*$  of an ensemble of particles is given by the sum of their kinetic energies  $E_k$  and their rest mass energies  $E_r = mc^2$ ; here  $m$  is the rest mass of the particle and  $c$  is the speed of light in free space. The total energy of an assembly of particles, for which we add the asterisk notation, is

therefore

$$E^* = \sum_j (E_{k,j} + E_{r,j}) = \sum_j (E_{k,j} + m_j c^2). \quad (1.12)$$

For the nuclear reaction of Eq.(1.7) we write the total energy—which must be conserved—as

$$E_{\text{before}}^* = E_{\text{after}}^* \quad (1.13a)$$

and hence

$$(E_{k,a} + m_a c^2) + (E_{k,b} + m_b c^2) = (E_{k,d} + m_d c^2) + (E_{k,e} + m_e c^2). \quad (1.13b)$$

Rearrangement of these terms yields

$$(E_{k,d} + E_{k,e}) - (E_{k,a} + E_{k,b}) = [(m_a + m_b) - (m_d + m_e)] c^2. \quad (1.14)$$

This important equation relates the difference in kinetic energies—before and after the collision—to their corresponding differences in rest masses; thus, as shown, a change in kinetic energy is related to a change in rest masses. Particle rest masses have been measured to a very high degree of accuracy allowing therefore the ready evaluation of the right-hand part of this equation. This defines the Q-value of the reaction

$$Q_{ab} = [(m_a + m_b) - (m_d + m_e)] c^2 = -[(m_d + m_e) - (m_a + m_b)] c^2 \quad (1.15a)$$

and represents the quantity of energy associated with the mass difference before and after the reaction. Hence, we may write more compactly

$$Q_{ab} = (-\Delta m)_{ab} c^2 \quad (1.15b)$$

where  $\Delta m$  is the mass decrement (i.e.  $\Delta m = m_{\text{after}} - m_{\text{before}}$ ) for the reaction. Evidently,  $Q_{ab}$  is positive if  $(\Delta m)_{ab} < 0$  and negative otherwise; the former case—involving a decrease of mass in the process—constitutes an exoergic reaction and the latter may be termed endoergic. Further, for the case of  $Q_{ab} < 0$ , the kinetic energy of the reaction-initiating particle must exceed this value before a reaction can be induced; that is, a threshold energy has to be overcome before the reaction will proceed.

Equation (1.15b) is a form of the famous relation

$$E = mc^2 \quad (1.16)$$

and asserts—as first proposed by Einstein—that matter and energy are equivalent. As a consequence, we may assert that if processes occur which release energy of amount  $E$ , then a corresponding decrease in rest mass of amount  $(-\Delta m)$  must have taken place.

### 1.3 Component Energies

A detailed kinematics characterization of reaction (1.7) requires the specification of both the kinetic energy and the momentum of the initial state of the reactants a and b as well as—depending upon the reaction details desired—the appropriate

field forces which may act on the particles. However, some useful relations about the energies of the reaction products d and e can be obtained for the simple case in which the reacting particles possess negligible kinetic energies relative to the Q-value of the reaction, i.e.  $E_{k,a} + E_{k,b} \ll Q_{ab}$ , and in which the total energy liberated is shared by the two reaction products d and e in the form of their kinetic energy. Under these conditions, Eqs.(1.14) and (1.15a) give

$$\frac{1}{2} m_d v_d^2 + \frac{1}{2} m_e v_e^2 \approx Q_{ab}. \quad (1.17a)$$

Then, restricting this analysis to the case that the centre of mass be at rest, Fig.1.2, momentum conservation provides for

$$m_d v_d = m_e v_e. \quad (1.17b)$$

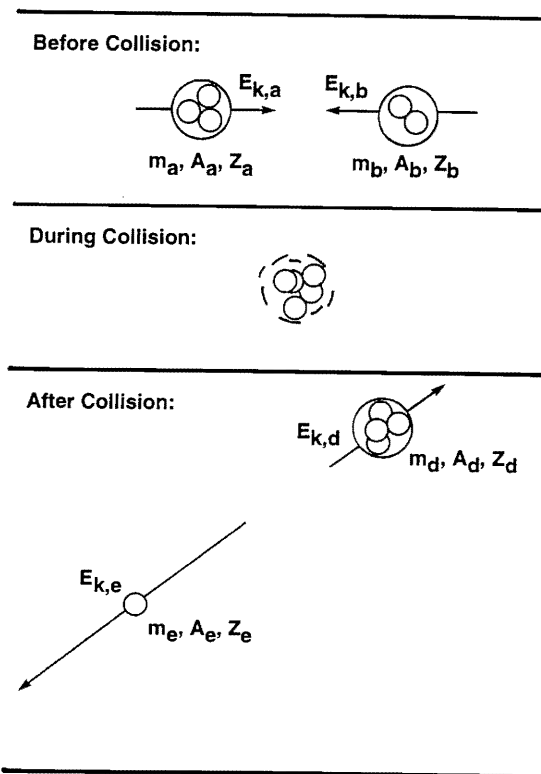


Fig. 1.2: Kinematic depiction of a head-on nuclear fusion reaction with the centre of mass at rest.

Solving Eq. (1.17b) for either  $v_d$  or  $v_e$  and substituting into Eq. (1.17a) yields kinetic energies  $E_{k,d}$  and  $E_{k,e}$  for the two reaction products:

$$E_{k,d} \approx \left( \frac{m_e}{m_d + m_e} \right) Q_{ab}, \quad E_{k,e} \approx \left( \frac{m_d}{m_d + m_e} \right) Q_{ab}. \quad (1.18)$$

For the specific case of d-t fusion, Eq. (1.5), for which  $Q_{dt} = 17.6$  MeV, the neutron and alpha particle kinetic energies are therefore found to be

$$E_{k,n} \approx \frac{4}{5} Q_{dt} \approx 14.1 \text{ MeV}, \quad E_{k,\alpha} \approx \frac{1}{5} Q_{dt} \approx 3.5 \text{ MeV}. \quad (1.19)$$

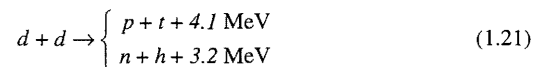
Thus, an 80 - 20% energy partitioning occurs between the reaction products.

## 1.4 Fusion Fuels

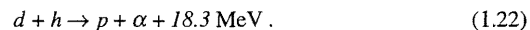
Observations of natural and induced processes have shown that numerous types of fusion reactions for which  $Q > 0$  can be identified. The variables for different reactions are the interacting nuclides\*, the reaction products which emerge, the Q-value of the reaction, and the dependence of the probability for the reaction to take place on the kinetic energy of the reactants. The fusion reaction most readily attainable under laboratory conditions and which is expected to be the first used for power generation purposes is the d-t reaction



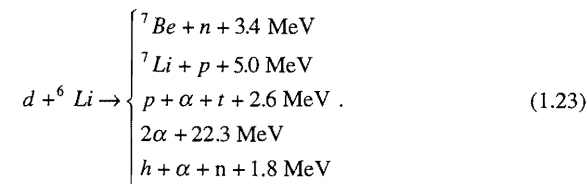
Another most accessible fusion reaction involves deuterium nuclei as fuel:



where h is chosen to represent the helium-3 nucleus ( ${}^3\text{He}^{2+}$ ). This representation may appear somewhat unusual, but is seen to simplify notation in subsequent chapters. Equation (1.21) shows that d-d will fuse via two distinct reaction channels known to occur with almost equal probabilities at specific reaction conditions. Further, fuel deuterons may also fuse with two of the reaction products (tritons and helium-3) giving, in addition to the reactions of Eqs. (1.21) and (1.20),

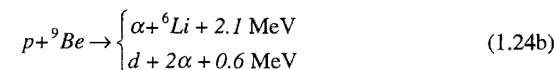


The above fusion reactions involve deuterons and the successively more massive light nuclides. Continuing along this pattern, a large number of reaction channels have been identified in specific cases of which d- ${}^6\text{Li}$  fusion is an example:

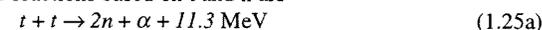


Here, each reaction channel possesses a unique probability of occurrence.

Fusion reactions involving the lightest nucleus, that is the proton, may occur according to the processes



as well as others. Some reactions based on t and h are



and



Several features associated with fusion reactions need to be noted. First, the physical demonstration of a fusion reaction is not the only consideration determining its choice as a fuel in a fusion reactor. Other considerations include the difficulty of bringing about such reactions, the availability of fusion fuels, and the requirements for attaining a sufficient reaction rate density.

Another feature of the various fusion reactions listed above needs to be emphasized: in each case a different fraction of the reaction Q-value resides in the kinetic energy of the reaction products. Thus, a fusion reactor concept based on high-efficiency direct energy conversion of charged particles would appear particularly suitable for those reactions which are characterized by a high fraction of the Q-value residing in the kinetic energy of the charged particles. This is of particular interest because the neutrons appearing as fusion reaction products invariably induce radioactivity in the materials surrounding the fusion core.

Third, the fusion fuels are evidently the light nuclides displayed on the Chart of the Nuclides. In a subsequent chapter we will show that a subatomic short-lived particle called a muon and produced in special accelerators, may also play a role as a fusion reaction catalyst.

Most current fusion research and development activity is based on the expectation that the d-t reaction, Eq. (1.20), will be used for the first generation fusion reactors. While the world's oceans as well as fresh water lakes and rivers contain an ample supply of deuterium with a particle density ratio of  $d/(p+d) \sim 1/6700$ , tritium is scarce; it is a radioactive beta emitter with a half life of 12.3

\* Appendix B displays the light-nuclide part of the Chart of the Nuclides.

years, with the total steady state atmospheric and oceanic quantity of tritium produced by cosmic radiation estimated to be on the order of 50 kg. Since a 1000 MW<sub>i</sub> plant will burn about 250 g of tritium each operating day, a station inventory in excess of 10 kg will be required for every d-t based central-station fusion power plant so that other sources of tritium fuel are required.

The main source of tritium is expected to be its breeding by capture of the fusion neutron in lithium contained in a blanket surrounding the fusion core. The relevant reactions in <sup>6</sup>Li and <sup>7</sup>Li are



and



with the latter possessing a high energy threshold  $E_{\text{thresh}} \approx 2.47$  MeV. Lithium-6 and lithium-7 are naturally occurring stable isotopes existing with 7.5% and 92.5% abundance, respectively, and exist terrestrially in considerable quantity.

Additional sources of tritium may involve its extraction from the coolant and moderator of existing fission reactors, particularly heavy water reactors, where tritium is incidentally produced by neutron capture in deuterium via



Of course, tritium could also be produced by placing lithium into control and shim rods of fission reactors.

Reaction (1.26b) is particularly interesting because the inelastically scattered neutron appearing at lower energy can continue to breed more tritium. Thus, in principle, it could be possible in such a system to produce more than 1 triton per neutron born in the d-t reaction. Indeed, present concepts for d-t reactors generally assume a lithium-based blanket surrounding the fusion core that allows for tritium self-sufficiency. These and additional concepts will be discussed in subsequent chapters.

## 1.5 Fusion in Nature

While a very small number of fusion reactions occur naturally under existing terrestrial conditions, the most spectacular steady state fusion processes occur in stellar media. Indeed, the formation of elements and the associated nuclear energy releases are conceived of as occurring in the burning of hydrogen during the gravitational collapse of a stellar proton gas; the initiating fusion process is

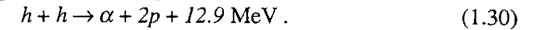


where  $\beta^+$  represents a positron and  $\nu$  a neutrino. Then, the deuteron thus formed may react with a background proton according to



Subsequently, this helium-3 reaction product could fuse with another helium-3

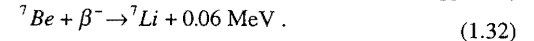
nucleus to yield an alpha particle and two protons:



The next heavier element is beryllium, produced by

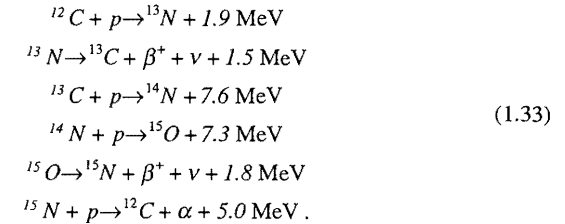


and is an example of a rare helium-4 fusion reaction. Also, lithium may appear by



A progression towards increasingly heavier nuclides is thus evident. This process is known as nucleosynthesis and provides a characterization for the initial stages of formation of all known nuclides.

Closed fusion cycles have also been identified of which the Carbon cycle is particularly important:



This sequence of linked reactions is graphically depicted in Fig.1.3 and may be collectively represented by



if all the reactions of Eq. (1.33) proceed at identical rates. This relation suggests that protonium burns due to the catalytic action of the isotopes <sup>12</sup>C, <sup>13</sup>C, <sup>13</sup>N, <sup>14</sup>N, <sup>15</sup>N, and <sup>15</sup>O.

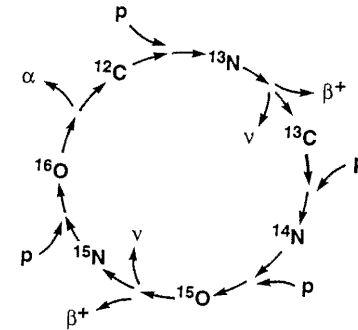


Fig. 1.3: Graphical depiction of the Carbon fusion cycle.

## Problems

1.1 Determine the energy released per mass-of-atoms initially involved for a chemical process, Eq.(1.2), for nuclear fission, Eq.(1.3), for nuclear fusion, Eq.(1.5) and for a water molecule falling through a 100 m elevation difference in a hydroelectric plant.

1.2 Calculate the reaction Q-values for each of the two branches of the d-d fusion reaction, Eq.(1.21).

1.3 What fraction of the original mass in d-t fusion is actually converted into energy? Compare this to the case of nuclear fission, Eq.(1.3).

1.4 Calculate the kinetic energies of the reaction products h and a resulting from p-<sup>6</sup>Li fusion, Eq.(1.24a), ignoring any initial motion of the reactants.

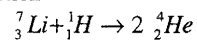
1.5 Calculate the total fusion energy, in Joules, residing in a litre of water if all the deuterons were to fuse according to Eq.(1.21).

1.6 Redo problem 1.5 including the burning of the bred tritium according to Eq. (1.20).

1.7 Consult an astronomy text in order to estimate the mean fusion power density ( $\text{Wm}^{-3}$ ) in the sun; compare this to a typical power density in a fission reactor.

1.8 The first artificial nuclear transmutation without the use of radioactive substances was successfully carried out in the Rutherford Laboratory by Cockcroft and Walton when they bombarded Lithium (at rest) with 100 keV proton canal rays (protons accelerated by a voltage of 100 kV and passing through a hole in the cathode). By scintillations in a Zincblende-screen, the appearance of  $\alpha$ -particles with a kinetic energy of 8.6 keV was determined.

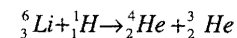
(a) Formulate the law of energy conservation valid for the above experiment referring to the nuclear reaction



and find therefrom the reaction energy,  $Q_{p7\text{Li}}$ , via the involved rest masses ( $m_p$ ,  $m_\alpha = 6.64455 \times 10^{-27}$  kg,  $m_{7\text{Li}} = 11.64743 \times 10^{-27}$  kg).

(b) In the Cockcroft-Walton experiment, conservation of momentum was proven by cloud chamber imaging whereby it was observed that the tracks of the two  $\alpha$ -particles diverge at an angle of  $175^\circ$ . What angle follows from the law of momentum conservation by calculation?

(c) A further reaction induced by the protons in natural lithium is



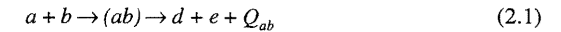
Provide an argument that shows the  $\alpha$ -particles detected in the Cockcroft-Walton experiment cannot stem from this reaction.

## 2. Physical Characterizations

A number of fusion reactions of interest were listed in the preceding chapter but little reference was made to the conditions under which these reactions might occur. We now consider the fusion process itself and some characterizations of conditions which are fundamental to an understanding of controlled nuclear fusion.

### 2.1 Particles and Forces

The general fusion reaction, Eq.(1.7) and Fig.1.2, may be more completely characterized by noting that an unstable intermediate state may be identified in nuclear reactions. That is, we should write



where (ab) identifies a complex short-lived dynamic state which disintegrates into products d and e. The energetics are determined according to nucleon kinetics analysis, with nuclear excitation and subsequent gamma ray emission known to play a comparatively small role in fusion processes at the energies of interest envisaged for fusion reactors.

Two-body interactions can be examined from various perspectives. For example, Newton's familiar law of gravitational attraction applies to any pair of masses  $m_a$  and  $m_b$  to yield a force

$$F_{g,a} = -G \frac{m_a m_b}{r^3} \mathbf{r} \quad (2.2)$$

effective on particle a. Here, G is the universal gravitational constant and  $\mathbf{r} = \mathbf{r}_a - \mathbf{r}_b$  is the displacement vector between the two interacting particles, while r denotes its absolute value. While this force expression is universal, a simple calculation will show that for nuclear masses of common interest, this force is significantly weaker than the electrostatic and nuclear forces associated with nuclides and hence can be neglected.

The important electrostatic force between two isolated particles of charge  $q_a$  and  $q_b$  separated by a distance r in free space is determined by Coulomb's law, given by

$$F_{c,a} = \frac{1}{4\pi \epsilon_0} \frac{q_a q_b}{r^3} \mathbf{r} \quad (2.3)$$

for the electrostatic force felt by particle a; here  $\epsilon_0$  is the permittivity of free space and the factor  $4\pi$  is extracted from the proportionality constant by reason of convention. This force—repulsive for like charges and attractive for unlike charges—is of considerable importance in fusion.

From the definition of work and the phenomenon of energy stored in a conservative field, the work done in moving a particle of charge  $q_a$  from a sufficiently distant point to within a distance  $r$  of a stationary charge of magnitude  $q_b$ , is the potential energy associated with the resultant charge configuration. Specifically, this is given by

$$\begin{aligned} U(r) &= \int_{\infty}^r \mathbf{F}_{ca}(\mathbf{r}') \cdot d\mathbf{r}' \\ &= \int_{\infty}^r \frac{1}{4\pi\epsilon_0} \frac{q_a q_b}{(r')^3} \mathbf{r}' \cdot d\mathbf{r}' \\ &= \int_{\infty}^r \frac{1}{4\pi\epsilon_0} \frac{q_a q_b}{(r')^3} (-r' dr') \\ &= \frac{1}{4\pi\epsilon_0} \frac{q_a q_b}{r} \end{aligned} \quad (2.4)$$

subject to the restriction that the particle distance of separation  $r$  satisfies  $r \geq R_a + R_b$  where  $R_a$  and  $R_b$  are the equivalent radii of the two charged particles. For nuclides of like charge, the potential energy at approximately the distance of "contact"  $R_0 = R_a + R_b$ , is called the Coulomb barrier and, in view of Eq.(2.4), is given by

$$U(R_0) = \frac{1}{4\pi\epsilon_0} \frac{q_a q_b}{(R_a + R_b)}. \quad (2.5)$$

On the basis of electrostatic considerations only, this then is the minimum kinetic energy an incident particle would have to possess in order to overcome electrostatic repulsion and come close enough to another particle for the short-range nuclear forces of attraction to dominate. For deuterium ions, this energy can be calculated to be about 0.4 MeV, depending upon the precise value for  $R_0$ . A useful approximation is  $R_0 \approx R_p(A_a^{1/3} + A_b^{1/3})$  where  $R_p = (1.3-1.7) \times 10^{-15}$  m denotes the radius of a proton which cannot be assigned a definite edge for quantum mechanical reasons.

Consideration of quantum mechanical tunneling provides for a non-vanishing probability of penetrating the Coulomb barrier with energies less than  $U(R_0)$ . The probability for this penetration varies as

$$Pr(\text{tunneling}) \propto \frac{1}{v_r} \exp\left(-\gamma \frac{q_a q_b}{v_r}\right) \quad (2.6)$$

where  $v_r$  is the relative speed of the moving particles and  $\gamma$  is a constant. Thus,

even at very low energy, a nucleus possesses a small, though finite, probability of compound formation with another nucleus. This compound can decay into fusion products and hence, some fusion reactions will also occur at room temperature, though at an insignificant rate.

At sufficiently small distances,  $r < R_0$ , the attractive strong nuclear force dominates and a compound nuclear state is formed. The kinetic energy of the initiating particles together with the resultant nuclear potential energy is then shared by all the nucleons. Nuclear stability considerations thereupon determine if and how the nucleus disintegrates. Figure 2.1 provides a graphical representation of these effects.

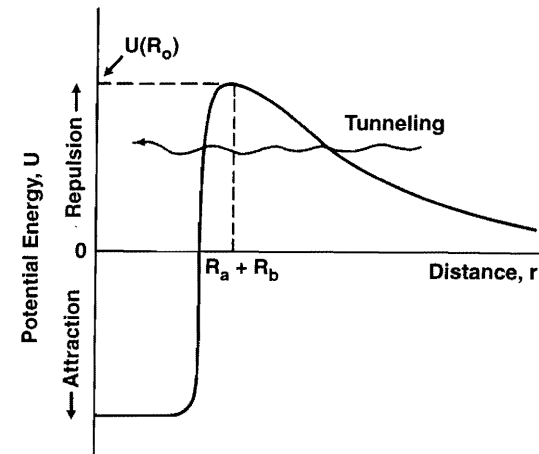


Fig. 2.1: Depiction of the ion-ion electrostatic repulsive potential for  $r > R_0$  and nuclear attraction for  $r < R_0$ .

## 2.2 Thermal Kinetics

The recognition that the Coulomb barrier for light ion fusion is in the 0.4 MeV range for the lightest known nuclides—p, d, and t—suggests that one approach to the attainment of frequent fusion reactions would be to heat a hydrogen gas up to a temperature for which a sufficient number of nuclei possess energies of relative motion in excess of  $U(R_0)$ , Eq.(2.5). However, because of the tunneling effect, such excessive heating is not required and substantial rates of fusion reactions are

achieved even when the average kinetic energy of relative motion of the reactant nuclei is in the tens-of-keV range. Note, however, that even providing such reduced conditions in a gas will be associated with heating up to temperatures near  $\sim 10^8$  K, for which, in recognition of the ionization potential of hydrogen being only 13.6 eV, the gas will completely ionize. The result therefore is an electrostatically neutral medium of freely moving electrons and positive ions called a plasma. With the average ion energy in a fusion reactor plasma thus allowed to be substantially less than the Coulomb barrier, the energy released from fusion reactions must exceed—for a viable energy system—the total energy initially supplied to heat and ionize the gas, and to confine the plasma thus produced. In practice, this means that when a sufficiently high plasma temperature has been attained, we have to sustain this temperature and confine the ions long enough until the total fusion energy released exceeds the total energy supplied. In subsequent chapters, we will consider some details of the relevant phenomena and processes and identify parametric descriptions of energy balances.

On the basis of the above considerations then, it is apparent that selected aspects of the classical Kinetic Theory of Gases, augmented by electromagnetic force effects, can be used as a basis for the study of a plasma in which fusion reactions occur. Thus, for the case of  $N$  atoms of proton number  $Z_i$ , complete ionization yields  $N_i$  ions and, in the case of charge neutrality,  $Z_i N_i = N_e$  electrons; that is

$$N \rightarrow N_i + N_e = N_i + Z_i N_i . \quad (2.7)$$

For hydrogenic atoms,  $Z_i = 1$  and hence  $N_e = N_i$ .

Often, the expression "Fourth State of Matter" is also assigned to such an assembly of globally neutral matter containing a sufficient number of charged particles so that the physical properties of the medium are substantially affected by electromagnetic interactions. Indeed, such a plasma may also exhibit collective behaviour somewhat like a viscous fluid and also possesses electrostatic characteristics of specified spatial dimension.

For a state of thermodynamic equilibrium, the Kinetic Theory of Gases asserts that the local pressure associated with the thermal motion of ions and electrons is given by

$$P_i = \frac{1}{3} N_i m_i \overline{v_i^2} \quad (2.8a)$$

and

$$P_e = \frac{1}{3} N_e m_e \overline{v_e^2} \quad (2.8b)$$

where the subscripts  $i$  and  $e$  refer to the ions and electrons respectively, and  $N_{( )}$  refers to the subscript-indicated particle population densities; note that it is the average of the squared velocity which appears as the important factor. The average kinetic energy of the electrons and ions can be introduced by simple algebraic manipulation of the above equations:

$$P_i = \frac{2}{3} N_i \left[ \frac{1}{2} m_i \overline{v_i^2} \right] = \frac{2}{3} N_i \overline{E}_i \quad (2.9a)$$

and

$$P_e = \frac{2}{3} N_e \left[ \frac{1}{2} m_e \overline{v_e^2} \right] = \frac{2}{3} N_e \overline{E}_e . \quad (2.9a)$$

Similar expressions may be written for the neutral particles in a plasma.

Accepting the kinetic theory of gases as a sufficiently accurate description allows for the use of well-known distribution functions. Implicit in this assumption is that the plasma under consideration is sufficiently close to thermodynamic equilibrium and that processes such as inelastic collisions, boundary effects and energy dependent removal of particles are of secondary importance.

The distribution functions for the particles of interest include dependencies on space, time and either velocity, speed or kinetic energy. Here we take a stationary ensemble of  $N^*$  particles uniformly distributed in space—either neutrals, ions or electrons—allowing us to write

$$N(\xi) = N^* M(\xi) \quad (2.10)$$

where  $\xi$  is one of the independent characteristic variables of motion— $v$ ,  $v$ , or  $E$ —and  $M(\xi)$  describes how the particles are distributed over the domain of this variable. Hence,  $N(\xi)$  is the distribution function of the ensemble of relevant particles in  $\xi$ -space and the symbol  $M()$  represents a normalized distribution function for the variable  $\xi$  such that

$$\int_{-\infty}^{\infty} M(\xi) d\xi = 1 \quad (2.11a)$$

with the integration performed over the entire definition range of the variable considered, i.e.

$$\int_{-\infty}^{\infty} M(v) dv = \int_0^{\infty} M(v) dv = \int_0^{\infty} M(E) dE = 1. \quad (2.11b)$$

Note that the particle number of the ensemble is given by

$$\int_{-\infty}^{\infty} N(\xi) d\xi = N^* \int_{-\infty}^{\infty} M(\xi) d\xi = N^* . \quad (2.12)$$

For a gas or, for the case of interest here, a plasma in thermodynamic equilibrium and in the absence of any field force effect, its particles of mass  $m$  moving in a sufficiently large volume follow the Maxwell-Boltzmann velocity distribution function given by

$$M(v) = \left( \frac{m}{2\pi kT} \right)^{3/2} \exp \left( \frac{-\frac{1}{2} m v^2}{kT} \right) . \quad (2.13)$$

Here  $k$  is the Boltzmann constant and  $T$  is the absolute temperature for the

ensemble. For the case of isotropy, the Maxwellian distribution of speeds is a generally satisfactory characterization and is given by

$$M(v) = \left(\frac{2}{\pi}\right)^{1/2} \left(\frac{m}{kT}\right)^{3/2} v^2 \exp\left(-\frac{1}{2} \frac{mv^2}{kT}\right), \quad 0 < v < \infty. \quad (2.14)$$

Finally, the corresponding distribution of particles in kinetic energy space  $E$  is described by the Maxwell-Boltzmann distribution

$$M(E) = \frac{2}{\sqrt{\pi}} \left(\frac{1}{kT}\right)^{3/2} E^{1/2} \exp\left(-\frac{E}{kT}\right), \quad 0 < E < \infty. \quad (2.15)$$

These three functions are illustrated in Fig.2.2.

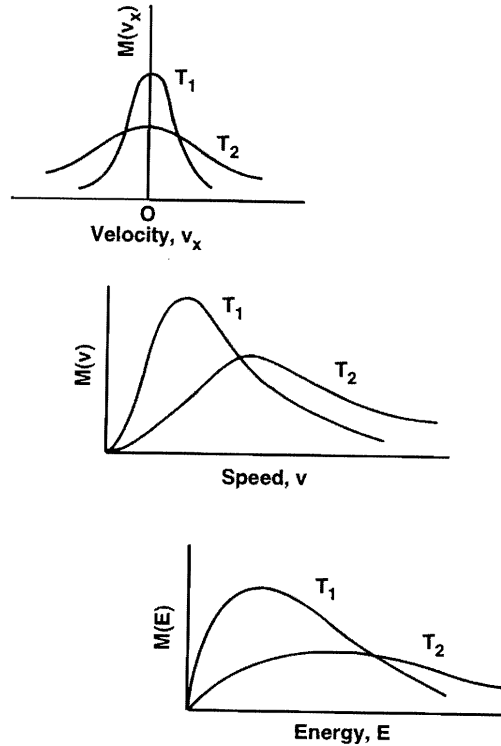


Fig. 2.2: Schematic depiction of the Maxwell-Boltzmann distribution functions for  $v_x$ ,  $v$  and  $E$  as independent variables; in each case,  $T_1 < T_2$ .

### 2.3 Distribution Parameters

It is most important to recognize that while the particles possess a range of velocities, speeds, and energies, the temperature  $T$  describes a particular distribution function and is a fixed parameter for a given thermal state; changing the temperature of the medium will alter the various moments of the function but its characteristic shape is retained, Fig.2.2.

Further, in a volume domain containing a mixture of particles—as in the case of a plasma containing electrons, various ion species, and neutrals—each particle species may possess a different distribution function characterized by a different temperature. Then, however, the entire plasma is not in thermodynamic equilibrium. Indeed, in the presence of a magnetic field, even the same species may have a different temperature in, say, the direction parallel to the magnetic field lines than in the perpendicular direction. Several methods or devices used to obtain fusion energy involve plasmas that are just that—not in thermodynamic equilibrium. Most that will be considered herein, however, are not so and thus we will rely on Maxwell-Boltzmann distributions to characterize many of the plasmas that will be discussed in subsequent chapters.

Having a sufficiently accurate distribution function is of considerable utility.

For example, the most probable value  $\xi$ —that is the peak of the distribution—is found by differentiating and finding the root of

$$\left. \frac{\partial M(\xi)}{\partial \xi} \right|_{\xi=\hat{\xi}} = 0. \quad (2.16)$$

For the three distribution functions listed, Eqs. (2.13), (2.14) and (2.15), this yields the following:

$$\left. \frac{\partial M(v)}{\partial v_x} \right|_{v_x=\hat{v}_x} = 0, \quad \hat{v}_x = 0 \quad (2.17a)$$

$$\left. \frac{dM(v)}{dv} \right|_{v=\hat{v}} = 0, \quad \hat{v} = \left(\frac{2kT}{m}\right)^{1/2} \quad (2.17b)$$

and

$$\left. \frac{dM(E)}{dE} \right|_{E=\hat{E}} = 0, \quad \hat{E} = \frac{1}{2} kT. \quad (2.17c)$$

In Eq. (2.17a), the subscript  $x$  is to suggest any one component of the vector  $v$ ; hence  $\hat{v} = \mathbf{0}$ .

Average values can similarly be found based upon the formal definition of

$$\bar{\xi} = \frac{\int \xi M(\xi) d\xi}{\int M(\xi) d\xi}. \quad (2.18)$$

Thus, for the three cases of interest here we get

$$\bar{v}_x = \int_{-\infty}^{\infty} v_x M(\mathbf{v}) dv_x = 0 \quad (\text{i.e. } \bar{\mathbf{v}} = \mathbf{0}) \quad (2.19a)$$

$$\bar{v} = \int_0^{\infty} v M(v) dv = \left( \frac{8kT}{m\pi} \right)^{1/2} \quad (2.19b)$$

and

$$\bar{E} = \int_0^{\infty} EM(E) dE = \frac{3}{2} kT \quad (2.19c)$$

with the particles possessing three degrees of freedom.

The analysis leading to the depictions of Fig. 2.2 makes it clear that the temperature  $T$ —here in units of degrees Kelvin,  $K$ —is an essential characterization of a Maxwellian distribution; hence, the numerical value of  $T$  uniquely specifies an equilibrium distribution. It has also become common practice to multiply  $T$  by the Boltzmann constant  $k$  and to call this product the kinetic temperature, which is obviously expressed in units of energy, either Joules (J) or electron volts (eV) with the latter generally preferred. Using this product  $kT$ , a Maxwellian population at  $T = 11,609 \text{ K}$  may be said to possess a kinetic temperature of 1 eV; similarly, a 3 keV plasma in thermodynamic equilibrium has an absolute temperature of  $3.48 \times 10^7 \text{ K}$ .

The convention of interchangeably using energy and temperature, wherein the adjective "kinetic" and Boltzmann's constant in  $kT$  are commonly suppressed, may seem peculiar, but expressing a physical variable in related units is a very common practice. For example, travelers often use time as a measure of distance ( $s = vt$ ) if the speed of transport is understood, test pilots often speak of a force of so many  $g$ 's ( $F = mg$ ), and physicists often quote rest masses in units of energy ( $E = mc^2$ ).

This convention of using the product  $kT$  leads to a number of uses which need to be distinguished; we note here several common cases:

$kT$  = (kinetic) temperature of a plasma;

$\frac{3}{2} kT$  = average energy of Maxwellian-distributed particles;

$\frac{1}{2} kT$  = most frequently occurring particle energy of Maxwellian-distributed particles;

$\sqrt{\frac{8}{m\pi}} \sqrt{kT}$  = average particle speed of Maxwellian-distributed particles.

## 2.4 Power and Reaction Rates

The power in a fusion reactor core is evidently governed by the fusion reaction rate. If only one type of fusion process occurs and if this process occurs at the

rate density  $R_{fu}$  with  $Q_{fu}$  units of energy released per reaction then the fusion power generated in a unit volume is given by

$$P_{fu} = R_{fu} Q_{fu} \quad (2.20)$$

With  $R_{fu}$  expressed in units of reactions  $\cdot m^{-3} \cdot s^{-1}$  and  $Q_{fu}$  in MeV per reaction, the units of the power density  $P_{fu}$  are  $MeV \cdot m^{-3} \cdot s^{-1}$  which can be converted to the more commonly used unit of Watt (W) by the conversion relationship  $1 eV \cdot s^{-1} = 1.6 \times 10^{-19} \text{ W}$  since  $1 \text{ W} = 1 \text{ J} \cdot s^{-1}$ . For the case of a uniform power distribution the total energy released during a time interval  $\tau$  in some volume  $V$  follows from Eq.(2.20) as

$$E_{fu}^* = V \int_0^{\tau} P_{fu} dt \quad (2.21a)$$

and, at any time  $t$

$$P_{fu} = \left( \frac{dE_{fu}^*}{dt} \right) \frac{1}{V} \quad (2.21b)$$

That is, energy may be viewed as the area under the power curve while power may be interpreted as an instantaneous energy current.

The energy generated in a given fusion reaction,  $Q_{fu}$  in Eq.(2.20), is the "Q-value" of the reaction, Eq.(1.15), and can be experimentally determined or extracted from existing tables; this part of the power expression is simple. However, the determination of the functional form of the reaction rate density  $R_{fu}$  is more difficult but must be specified if the fusion power  $P_{fu}$  is to be computed.

In order to determine an expression for the fusion reaction rate density, consider first the special case of two intersecting beams of monoenergetic particles of type  $a$  and type  $b$  possessing number densities  $N_a$  and  $N_b$ , respectively, Fig. 2.3.

In a unit volume where the two beams intersect, the number of fusion events in a unit volume between the two types of particles, at a given time, is given by a proportionality relationship of the form

$$R_{fu} \propto N_a N_b v_r \quad (2.22)$$

where  $v_r$  is the relative speed of the two sets of particles at the point of interest. This relation is based on a heuristic plausibility argument for binary interactions. Obviously, some idealizations are contained in Fig.2.3 and Eq.(2.22), such as particles of varying energy and direction of motion as well as the interaction of particles with others of their species not being accounted for, but will be considered in subsequent sections.

The proportionality relationship of Eq.(2.22) can be converted into an explicit equation by the introduction of a proportionality factor represented here by  $\sigma_{ab}$  for a given  $v_r$ :

$$R_{fu} = \sigma_{ab}(v_r) N_a N_b v_r \quad (2.23)$$

The subscript  $ab$  and the functional dependence on  $v_r$ , indicated in  $\sigma_{ab}(v_r)$ , is to emphasize that the magnitude of this parameter is specifically associated with the particular types of interacting particles and their relative speed. The common name for  $\sigma_{ab}(v_r)$  is "cross section" and, since all the terms of Eq.(2.23) are already dimensionally specified, its units are those of an area. This parameter has been assigned the name "barn", abbreviated  $b$ , and defined as

$$1 \text{ b} = 10^{-24} \text{ cm}^2 = 10^{-28} \text{ m}^2. \quad (2.24)$$

Figure 2.4 illustrates the cross section for a case of deuterium-tritium fusion. Note a maximum of a few barns in the  $v_r = 3 \times 10^6 \text{ ms}^{-1}$  range in this figure.

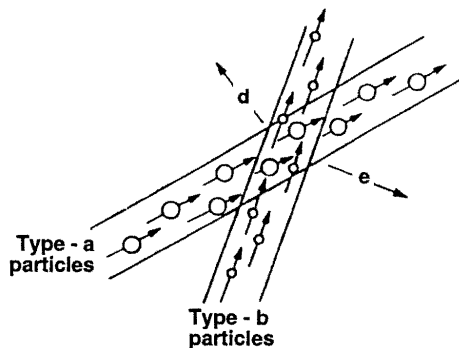


Fig. 2.3: Intersection of two particle beams resulting in fusion reactions  $a + b \rightarrow d + e$ .

## 2.5 Sigma-V Parameter

The fusion reaction rate density expression of Eq.(2.23) is very restrictive since all particles were taken to possess a constant speed and their motion was assumed to be monodirectional. However, the general case of an ensemble of particles possessing a range of speeds and moving in various directions can be introduced by extending Eq.(2.23) to include a summation over all particle energies and all directions of motion. The integral calculus is ideally suited for this purpose requiring, however, that we redefine some terms. Letting therefore the particle densities be a function of velocity  $\mathbf{v}$  endows them with a range of energies and range of directions; that is, we progress from simple particle densities which give the number of particles per unit volume, to distribution functions describing how many particles in a considered position interval move with a certain velocity, according to

$$N_a \rightarrow N_a(\mathbf{v}_a) = N_a F_a(\mathbf{v}_a) \quad (2.25a)$$

and

$$N_b \rightarrow N_b(\mathbf{v}_b) = N_b F_b(\mathbf{v}_b). \quad (2.25b)$$

The terms which have replaced the previous particle densities are distributions in the so-called position-velocity phase space. Thus, the velocity distribution functions  $F_a(\mathbf{v}_a)$  and  $F_b(\mathbf{v}_b)$  satisfy the normalization

$$\int_{\mathbf{v}_a} F_a(\mathbf{v}_a) d^3 \mathbf{v}_a = 1, \quad (2.26a)$$

as well as

$$\int_{\mathbf{v}_b} F_b(\mathbf{v}_b) d^3 \mathbf{v}_b = 1. \quad (2.26b)$$

Here  $d^3 v_{( )}$  is to indicate integration over the three velocity components. Hence, though we show here only one integral, the implication is that for calculational purposes there will be as many integrals as there are scalar components for each of the vectors  $\mathbf{v}_a$  and  $\mathbf{v}_b$ .

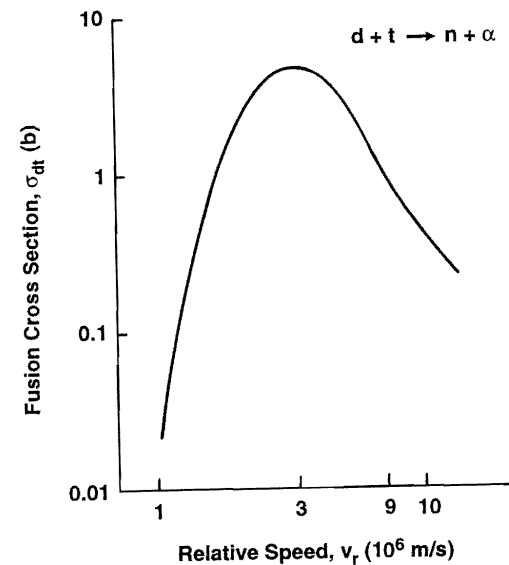


Fig. 2.4: Fusion cross section for a deuterium beam incident on a tritium target.

The relative speed of two interacting particles at a point of interest is, by its usual definition, given as

$$v_r = |\mathbf{v}_a - \mathbf{v}_b|. \quad (2.27)$$

Finally then, a general rate density expression for binary reactions follows by extension of Eq.(2.23) over the corresponding velocity space:

$$\begin{aligned} R_{fu} &= \int \int_{\mathbf{v}_a \mathbf{v}_b} \sigma_{fu}(|\mathbf{v}_a - \mathbf{v}_b|) |\mathbf{v}_a - \mathbf{v}_b| N_a F_a(\mathbf{v}_a) N_b F_b(\mathbf{v}_b) d^3 v_a d^3 v_b \\ &= N_a N_b \int \int_{\mathbf{v}_a \mathbf{v}_b} \sigma_{fu}(|\mathbf{v}_a - \mathbf{v}_b|) |\mathbf{v}_a - \mathbf{v}_b| F_a(\mathbf{v}_a) F_b(\mathbf{v}_b) d^3 v_a d^3 v_b. \end{aligned} \quad (2.28)$$

By first impressions, this double integral appears formidable, particularly when it is realized that the vectors  $\mathbf{v}_a$  and  $\mathbf{v}_b$  possess, in general, three components so that a total of six integrations are required. However, aside from any algebraic or numerical problems of evaluation, this integral contains two important physical considerations. First, the cross section  $\sigma_{fu}(|\mathbf{v}_a - \mathbf{v}_b|)$  must be known as a function of the relative speed of the two types of particles, and second, the distribution functions  $F_i(\mathbf{v}_i)$  must be known for both populations of particles.

We note however that Eq.(2.28) possesses all the properties of an averaging process in several dimensions; that is, it represents averaging the product  $\sigma_{ab}(|\mathbf{v}_a - \mathbf{v}_b|) |\mathbf{v}_a - \mathbf{v}_b|$  with two normalized weighting functions  $F_a(\mathbf{v}_a)$  and  $F_b(\mathbf{v}_b)$  over all velocity components of  $\mathbf{v}_a$  and  $\mathbf{v}_b$ . Such averaging yields the definition

$$\langle \sigma v \rangle_{ab} = \int \int_{\mathbf{v}_a \mathbf{v}_b} \sigma_{ab}(|\mathbf{v}_a - \mathbf{v}_b|) |\mathbf{v}_a - \mathbf{v}_b| F_a(\mathbf{v}_a) F_b(\mathbf{v}_b) d^3 v_a d^3 v_b. \quad (2.29)$$

This parameter, here named sigma-v (pronounced "sigma-vee"), is often also called the reaction rate parameter. Note the implicit dependence on temperature via the distribution functions  $F_a(\mathbf{v}_a)$  and  $F_b(\mathbf{v}_b)$  so that  $\langle \sigma v \rangle_{ab}$  is a function of temperature.

The reaction rate density involving two distinct types of particles a and b, Eq.(2.28), is therefore written in compact form as

$$R_{fu} = N_a N_b \langle \sigma v \rangle_{ab}. \quad (2.30)$$

This sigma-v parameter for the case of d-t fusion under conditions in which both the deuterium and tritium ions possess a Maxwellian distribution, that is  $F_i(\mathbf{v}_i) \rightarrow M_i(\mathbf{v}_i)$  in Eq.(2.29), and where both species possess the same temperature, is depicted in Fig.2.5.\* Note that generally  $\langle \sigma v \rangle_{ab}$  will also be a function of space and time because the velocity distributions may also depend upon these variables.

We make two additional comments about the reaction rate density expression, Eq.(2.30). First, the assumption of Maxwellian distributions, i.e.

\* Appendix C provides a tabulation of this and other  $\langle \sigma v \rangle_{ab}$  parameters.

$F_i(\mathbf{v}_i) \rightarrow M_i(\mathbf{v}_i)$  as discussed in Sec.2.3, is very frequently made in tabulations of sigma-v; the reason for this is because many approaches to the attainment of fusion energy rely upon the achievement of plasma conditions that are close to thermodynamic equilibrium. For cases where equilibrium conditions do not exist, the appropriate distribution functions  $F_a(\mathbf{v}_a)$  and  $F_b(\mathbf{v}_b)$  must be determined and used in Eq.(2.29). For example, in some experiments, deuterium beams are injected into a tritiated target or into a magnetically confined tritium plasma to cause fusion by "beam-target" interactions. In such cases, one substitutes  $F_d(\mathbf{v}_d)$  by a delta distribution function at the velocity  $\mathbf{v}_b(t)$  characteristic of the instantaneous velocity of the beam ions slowing down in the plasma. However,  $F_t(\mathbf{v}_t)$  for the plasma target could well be assumed to be Maxwellian at the temperature of the tritium plasma. Then the averaged product of  $\sigma$  and  $v_r$  is often called the beam-target reactivity  $\langle \sigma v \rangle_{dt}^b$  for d-t fusion and is displayed in Fig.2.6; it appears to be a function of both the target temperature and the instantaneous energy of the slowing-down beam deuterons.

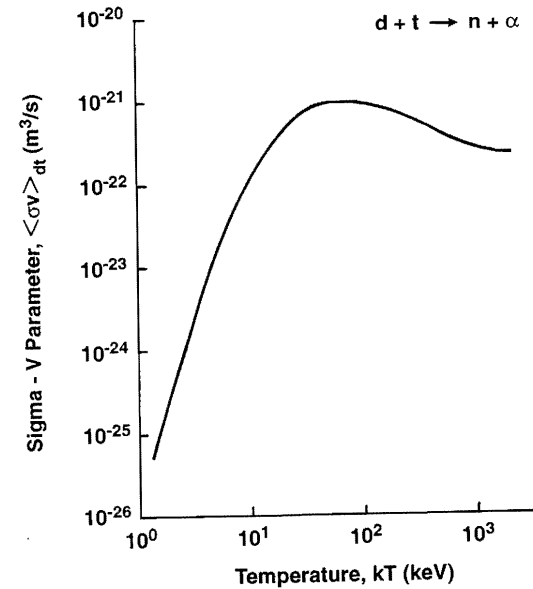


Fig. 2.5: Sigma-v parameter for d-t fusion in a Maxwellian-distributed deuterium and tritium plasma

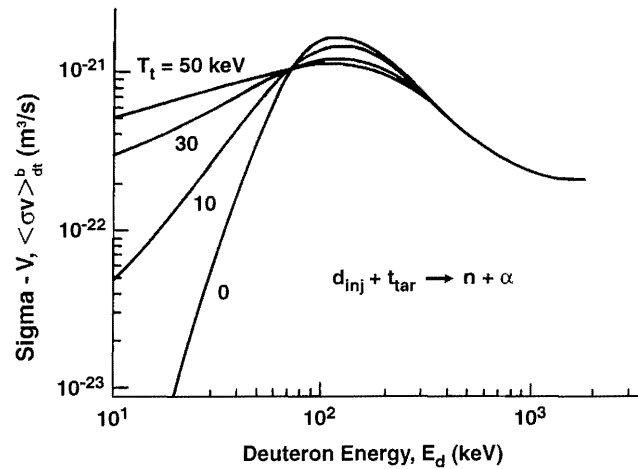


Fig. 2.6: Beam target sigma-v parameter for the case of deuterium injection into a tritium target of various temperatures.

Secondly, Eq.(2.30) assumes that the a-type and b-type particles are different nuclear species; the case when they might be indistinguishable is treated in a subsequent chapter where, in addition to d-t fusion, the case of d-d fusion is also considered.

A demonstration of the occurrence of fusion reactions is readily accomplished in a simple experiment employing a small accelerator which bombards a tritiated target with deuterium ions of such a high energy that during slowing down in the target they pass through the most favourable energy range for fusion; consider, in particular, the tritium plasma target of Fig.2.6 for this purpose. The appearance of neutrons and alphas as reaction products at the proper energies is then the proof of fusion events. The objective of fusion energy research and development is, however, the attainment of a sufficiently high fusion reaction rate density under controlled conditions subject to the overriding requirement that the power produced be delivered under generally acceptable terms. This is a considerable challenge and to this end a variety of approaches have been and continue to be pursued.

### Problems

2.1 Calculate the ratio of gravitational to electrical forces between a deuteron

### Physical Characterizations

- 2.2 Determine the Coulomb barrier for the nuclear reactions d-t, d-h, and p-<sup>11</sup>B.
- 2.3 Confirm the correctness of Eqs.(2.17) and (2.19).
- 2.4 For Maxwellian distributed tritons at 9 keV, calculate  
 (a) the average kinetic energy,  
 (b) the average speed, and  
 (c) the kinetic energy derived from the average speed of (b). Compare the energies of (a) and (c), and explain any difference.
- 2.5 Transform  $M(v)$ , Eq.(2.14), into  $M(E)$ , Eq.(2.15), with the aid of the appropriate Jacobian.
- 2.6 Find  $M(E)$  from  $M(v)$  for the case of isotropy using spherical coordinates.
- 2.7 Consult appropriate sources to determine particle densities  $N$  ( $m^{-3}$ ), the corresponding energies  $kT$  (eV) and temperatures  $T$  (K) for the following plasmas: outer space, a flame, the ionosphere, commonly attainable laboratory discharges and values expected in a magnetically as well as inertially confined fusion reactor. Plot these domains on an  $N$  vs.  $kT$  plane.

### 3. Charged Particle Scattering

A common approach to the achievement and sustainment of fusion reactions involves conditions in which the fuel mixture exists in a plasma state. Such a state of rapidly moving ions and electrons provides for extensive scattering due to Coulomb force effects. These are particularly important because they lead to kinetic energy variations amongst particles, and more importantly, to particle losses from the reaction region thereby affecting the energy viability of the plasma.

#### 3.1 Collisional Processes

Collisions between atomic, nuclear, and subnuclear particles take many forms. The important process of fusion between light nuclides represents a "discrete" inelastic process of nucleon rearrangement in which the reactants lose their former identity. In contrast, Coulomb scattering among ions and electrons causes "continuous" changes in direction of motion and kinetic energy. All these phenomena occur in a plasma to a varying extent and are therefore important in all confinement devices.

There may also exist a need to describe other selected collisional events in a fully or partially ionized medium, requiring therefore that the distinguishing characteristics of various processes be identified. Among these we note atomic processes such as photo-ionization, electron impact excitation, fluorescence, charge transfer and recombination, among others. Nuclear processes include inelastic nuclear excitation, nuclear de-excitation and elastic scattering.

A commonly occurring and important type of collision in a plasma is charged particle scattering attributable to the mutual electrostatic force. Such Coulomb scattering can vary from the most frequently occurring small-angle "glancing" encounters due to long-range interactions, up to the least likely near "head-on" collisions. The Coulomb scattering probability for ions is much larger than that to undergo fusion. Note that the deflections encountered in scattering reactions may lead to significant bremsstrahlung radiation power losses which lower the plasma temperature.

In general, the complete analysis of charged particle scattering is physically complex and mathematically tedious. As a consequence, we chose here to employ selected reductions in order to convey some of the essential and dominant features of specific relevance for our purposes here.

### 3.2 Differential Cross Section

Consider an isolated system of two ions of charge  $q_a$  and  $q_b$ , and possessing corresponding masses  $m_a$  and  $m_b$ . The magnitude of the Coulomb force is given by

$$F_c = \frac{1}{4\pi\epsilon_0} \frac{q_a q_b}{r^2} \quad (3.1)$$

where  $r$  is the distance of separation at any instant; evidently, as the charges move, this distance and also the direction of the force varies with time. The resultant trajectory of the particles  $a$  and  $b$  is suggested in Fig.3.1 for charged particle repulsion and attraction. In order to clearly specify a cross section for this process, it is useful to introduce the impact parameter  $r_o$  and the scattering angle  $\theta_s$  with respect to the initial and final asymptotic particle trajectories. In Fig. 3.1 the two colliding particles are shown in antiparallel motion because such a simplified situation always applies if the collision is analyzed in the centre of mass reference frame. Thus, the deflection angle  $\theta_s$  here indicated is identical to the scattering angle in the centre of mass system  $\theta_c$ , which is associated with the directional change of the relative velocity  $v_r$ , to be subsequently introduced. Intuition based on physical grounds suggests a rigid relationship between the three parameters  $r_o$ ,  $\theta_c$  and  $v_r$ .

For the case of azimuthally symmetric scattering, Fig. 3.2, and which here applies because of the specific form of  $F_c$ , every ion of mass  $m_b$  and charge  $q_b$  moving through the ring of area

$$dA = 2\pi r_o dr_o \quad (3.2)$$

will scatter off particle  $a$ —which has a charge of the same sign—through an angle  $\theta_c$  into the conical solid angle element  $d\Omega^*$  associated with the shadowed ring of Fig. 3.2; this conical solid angle element is evidently

$$d\Omega^* = 2\pi \sin(\theta_c) d\theta_c \quad (3.3)$$

The number of ions which scatter into a solid angle element can change substantially with  $r_o$  and  $v_r$ ; it is therefore necessary to look for an angle dependent cross section  $\sigma(\Omega)$  which here, due to azimuthal symmetry, is only a function of  $\theta_c$  and yields a total scattering cross section  $\sigma_s$  according to

$$\sigma_s = \int_0^{4\pi} \sigma_s(\theta_c) d^2\Omega = \int_0^\pi \sigma_s(\theta_c) d\Omega^* \quad (3.4)$$

implying the relation

$$\sigma_s(\theta_c) = \frac{d\sigma_s}{d\Omega^*} \quad (3.5)$$

That is,  $\sigma_s(\theta_c)$  is a function of the conical solid angle  $\Omega^*$  corresponding to a specified  $\theta_c$  and possesses units of barns per steradian (b/sr). Since  $d\sigma_s$  represents the differential cross sectional target area  $dA$  of Fig.3.2, and all ions entering this

area will depart through the solid angle element  $d\Omega^*$ , we may write

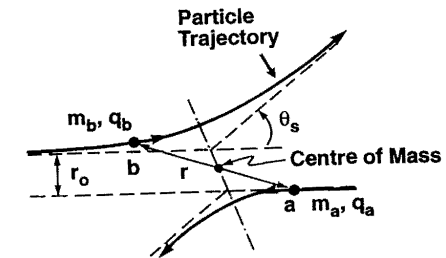
$$N 2\pi r_o dr_o = N \sigma_s(\theta_c) d\Omega^* \quad (3.6)$$

with  $N$  denoting a particle number per unit area, which, upon insertion of Eq.(3.3) yields specifically

$$\sigma_s(\theta_c) = \frac{r_o}{\sin(\theta_c)} \left| \frac{dr_o}{d\theta_c} \right| \quad (3.7)$$

where  $0 \leq \theta_c \leq \pi$ . Here, the standard absolute-value notation for the Jacobian of a transformation has been incorporated. The process discussed above refers to the so-called Rutherford scattering and  $\sigma_s(\theta_c)$  is known as the corresponding differential scattering cross section.

#### Case of Repulsion



#### Case of Attraction

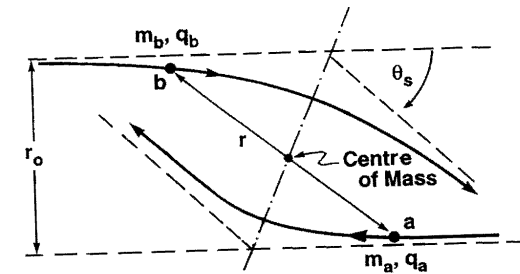


Fig. 3.1: Trajectories of ions "b" and "a" in the centre of mass reference frame under the influence of Coulomb repulsion and attraction.

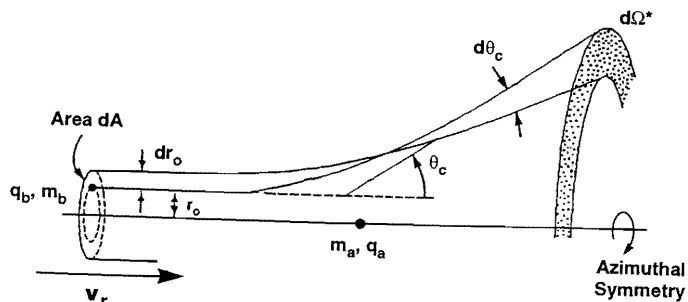


Fig. 3.2: Depiction of an ion b, moving within an area  $dA$  with speed  $v_r$  towards another ion a and being scattered into the solid angle  $d\Omega^*$ .

The functional relationship between the impact parameter  $r_o$  and the polar angle of scattering  $\theta_c$  needs to be determined before Eq.(3.7) can be specified.

The precise relationship between the impact parameter, the scattering angle, and the relative ion speed requires a detailed examination of the kinetics of the process together with the specification of energy and momentum conservation. These considerations and associated algebraic procedures are very cumbersome and will not be undertaken here. Suffice it to summarize that for the general case of arbitrary motion of two charged particles, the important relations can be compactly stated as

$$\tan\left(\frac{\theta_c}{2}\right) = \left(\frac{q_a q_b}{4\pi \epsilon_o}\right) \left(\frac{1}{m_r v_r^2 r_o}\right) \quad (3.8)$$

where the parameters introduced are as follows:

$\theta_c$  = scattering angle for particle b off of particle a in the COM (Centre of Mass) system which relates to  $\theta_L$  in the LAB (Laboratory) system according to

$$\cot(\theta_L) = \frac{m_b}{m_a} \csc(\theta_c) + \cot(\theta_c); \quad (3.9a)$$

$$m_r = \text{reduced mass of the two body system} \\ = (m_a m_b) / (m_a + m_b); \quad (3.9b)$$

$$v_r = \text{relative speed of the two particles of interest} \\ = |\mathbf{v}_a - \mathbf{v}_b|. \quad (3.9c)$$

The meaning of the impact parameter  $r_o$  is unchanged.

Equation (3.8) provides a useful connection between the impact parameter  $r_o$ , the scattering angle  $\theta_c$  in the COM system, and the relative particle speed  $v_r$ . For

simplicity, we may write

$$\tan\left(\frac{\theta_c}{2}\right) = \frac{K}{r_o}, \quad K = \frac{q_a q_b}{4\pi \epsilon_o m_r v_r^2} \quad (3.10)$$

with  $K$  thus a parameter of the charge, mass, and the kinetic state of the two collision partners. To complete Eq. (3.7), we recall our previous comment on the geometry-of-collision of interest, Fig. 3.1, which allows the scattering angle  $\theta_s$  introduced therein to be interchanged with  $\theta_c$ , and use Eq. (3.10) to determine  $dr_o/d\theta_c$  for  $K$  as a constant and thereby obtain the differential scattering cross section in the COM reference frame. That is, we get

$$\frac{1}{2} \sec^2\left(\frac{\theta_c}{2}\right) d\theta_c = -\frac{K}{r_o^2} dr_o \quad (3.11)$$

and hence

$$\left|\frac{dr_o}{d\theta_c}\right| = \frac{r_o^2}{2K} \sec^2\left(\frac{\theta_c}{2}\right). \quad (3.12)$$

Then, substitution of this expression in Eq.(3.7) gives

$$\sigma_s(\theta_c) = \left(\frac{r_o}{\sin(\theta_c)}\right) \left(\frac{r_o^2 \sec^2(\theta_c/2)}{2K}\right). \quad (3.13)$$

Now using Eq.(3.10) to eliminate the impact parameter  $r_o$  and employing the general half-angle identity

$$\sin(\theta) = 2\cos\left(\frac{\theta}{2}\right)\sin\left(\frac{\theta}{2}\right) \quad (3.14)$$

yields, upon algebraic simplification, the final expression of relevance:

$$\sigma_s(\theta_c) = \frac{K^2}{4 \sin^4(\theta_c/2)} = \frac{1}{4} \left(\frac{q_a q_b}{4\pi \epsilon_o m_r v_r^2}\right)^2 \frac{1}{\sin^4(\theta_c/2)} \quad (3.15)$$

This explicit algebraic form is frequently called the Rutherford scattering cross section.

The more significant information about this charged particle interaction cross section is suggested in Fig. 3.3 and illustrates the following important result: the cross section approaches  $\sigma_s(\theta_c) \rightarrow K^2/4$  for "head-on" collisions (i.e.  $r_o \rightarrow 0$ ) and becomes arbitrarily large for increasingly smaller "glancing" angles (i.e.  $r_o \rightarrow \infty$ ).

An informative conclusion about the singularity as  $\theta_c \rightarrow 0$  is that, for example, if there were to exist only two nonstationary charged particles in the universe then some deflection would occur with certainty regardless of how far apart they were; that is, the Coulomb  $1/r^2$  force dependence may become infinitesimally small at sufficient separations but, in principle, it never vanishes. Identifying a "reasonable" length beyond which charge effects can be considered to be unimportant, or even be ignored, is provided by the Debye length concept to be discussed next.

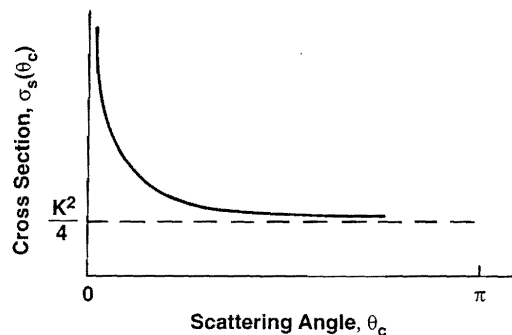


Fig. 3.3: Depiction of the Rutherford cross section as a function of scattering angle. Note  $\sigma_s(\theta_c) \rightarrow \infty$  as  $\theta_c \rightarrow 0$ .

### 3.3 Debye Length

Though a plasma is globally neutral, it may well acquire local charge variations which establish an electric potential and give rise to an electric field. The thermal motion of ions and electrons will therefore be influenced by the consequent force effects. An indication of the spatial extent of such an effect is represented by the Debye length. The following analysis yields a useful explicit expression for this important parameter.

Consider a dominant positive charge or electrode inserted in a plasma, Fig. 3.4. Due to the mobility of electrons, a negatively charged cloud will immediately form around this point with its density decreasing with distance. Similarly, a negative charge will also create a positive ion cloud spherically symmetric about it. Obviously, a plasma tends to shield itself from applied electric fields; that is, if an electrode is inserted into a plasma it will affect only its immediate surroundings. If the plasma were cold, one would observe as many charges in the surrounding cloud as are required to neutralize the inserted charge, Fig. 3.4. However, due to the finite plasma temperature, the plasma particles possess a substantial kinetic energy of thermal motion so that some—particularly those at the edge of the cloud—will escape from the shielding cloud by surmounting the electrostatic potential well which, as is known, decreases with increased distance  $r$ .

Evidently, we need to determine some characteristic shielding range and consider for that—over a small distance  $r$  from an inserted charge—some little

perturbation of the electric charge density in the plasma. Beyond this range, a uniform neutral plasma continues to reside. The local electric field  $\mathbf{E}$  thus established is related to the local charge density  $\rho^c$  by Maxwell's First Equation

$$\nabla \cdot \mathbf{E} = \frac{\rho^c}{\epsilon_0} \tag{3.16}$$

With this conservative field, a scalar potential function  $\Phi$  is identified and related to the electric field by

$$\mathbf{E} = -\nabla\Phi \tag{3.17}$$

By substitution in Eq.(3.16) and specializing for the case of interest, Fig. 3.4., Poisson's Equation takes on the form

$$\nabla \cdot (-\nabla\Phi) = \frac{\rho^c}{\epsilon_0} \tag{3.18}$$

which, upon introducing the definition

$$\rho^c = \sum_{j=e,i} q_j N_j \tag{3.19}$$

is written for a plasma containing only one species of ions as

$$-\nabla^2\Phi = \frac{q_e N_e + q_i N_i}{\epsilon_0} = \frac{-|q_e|}{\epsilon_0} (N_e - N_i) \tag{3.20}$$

in which  $q_i$  and  $q_e$  are the ion and electron charge, and  $N_i$  and  $N_e$  are the local ion and electron densities, respectively. Determining the potential function  $\Phi$  requires a knowledge of  $N_i$  and  $N_e$  as functions of position or of  $\Phi$ .

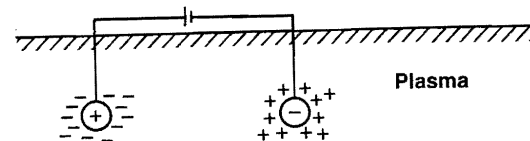


Fig. 3.4: Local charge variation in a plasma upon insertion of two dominant point charges.

The particle densities  $N_j$ , however, at thermodynamic equilibrium and in the presence of a potential energy  $\Phi$  are known to depend upon  $\Phi$ , the specific charge and the equilibrium temperature  $T_j$  according to the Boltzmann relation

$$N_e = C \exp\left(\frac{-q_e \Phi}{kT_e}\right) \tag{3.21a}$$

with the factors  $C_j$  being determined from the evident affinity  $\Phi \rightarrow 0$  as  $r \rightarrow \infty$  to represent the undisturbed background densities  $N_j(r \rightarrow \infty)$ . Equation (3.21a) may then be expanded by a Taylor series to give

$$N_e \approx N \left[ 1 + \frac{|q_e| \Phi}{kT_e} + \frac{1}{2} \left( \frac{|q_e| \Phi}{kT_e} \right)^2 \dots \right]. \quad (3.21b)$$

This refers to the region where  $|q_i \Phi / kT_i| \ll 1$ , which is actually the dominant contributor to the thickness of the shielding cloud. Retaining only the linear terms of the expansion and substituting into Eq. (3.20) yields

$$-\nabla^2 \Phi \approx \frac{-|q_e|}{\epsilon_0} \left[ N \left( 1 + \frac{|q_e| \Phi}{kT_e} \right) - N \right] = -\frac{|q_e| N}{\epsilon_0} \left( \frac{|q_e| \Phi}{kT_e} \right) \quad (3.22)$$

where we have used the charge-neutrality boundary condition

$$q_e N_e(r \rightarrow \infty) + q_i N_i(r \rightarrow \infty) = 0. \quad (3.23)$$

The defining equation for the electrical potential function  $\Phi$ , Eq. (3.22), is evidently of the form

$$\nabla^2 \Phi - \frac{\Phi}{\lambda_D^2} = 0 \quad (3.24)$$

with  $\lambda_D$  defined as the Debye length

$$\lambda_D = \sqrt{\frac{\epsilon_0 kT_e}{q_e^2 N}}. \quad (3.25)$$

Denoting the length for shielding ions by electrons by

$$\lambda_{De} = \sqrt{\frac{\epsilon_0 kT_e}{q_e^2 N_e(r \rightarrow \infty)}} \quad (3.26a)$$

and for screening electrons by ions by

$$\lambda_{Di} = \sqrt{\frac{\epsilon_0 kT_i}{q_i^2 N_i(r \rightarrow \infty)}} \quad (3.26b)$$

we realize the relation

$$\frac{1}{\lambda_D^2} = \frac{1}{\lambda_{De}^2} + \frac{1}{\lambda_{Di}^2}. \quad (3.27)$$

Taking  $T_e = T_i = T$  and assuming the presence of singly-charged ions only, that is  $N_i(r \rightarrow \infty) = N_e(r \rightarrow \infty) = N/2$ , notably simplifies Eq. (3.25) to the expression

$$\lambda_D = \sqrt{\frac{\epsilon_0 kT}{q_e^2 N}}. \quad (3.28a)$$

The important dependence of  $\lambda_D$  is therefore

$$\lambda_D \propto \sqrt{\frac{T}{N}} \quad (3.28b)$$

with typical values of interest to thermonuclear fusion being in the range of about

1  $\mu\text{m}$  to 1 mm.

The role of  $\lambda_D$  may be interpreted as a "shielding length" parameter for a plasma and becomes evident by solving Eq.(3.22) for the boundary conditions

$$\Phi(r=0) = \Phi_0 \quad \text{and} \quad \Phi(r \rightarrow \infty) = 0. \quad (3.29)$$

For the case of spherical geometry one obtains for the potential function in a plasma

$$\Phi_{\text{plasma}} \propto \frac{\exp(-r/\lambda_D)}{r} \quad (3.30a)$$

which may be compared to the free-space potential given by

$$\Phi_{\text{free space}} \propto \frac{1}{r}. \quad (3.30b)$$

Thus, the potential  $\Phi$  associated with the imposed electrostatic perturbation is attenuated in a plasma according to the magnitude of  $\lambda_D$  and is commonly said to be shielded to the distance of the Debye length.

This  $\lambda_D$  parameter is thus a useful concept and application of it relates to the elimination of the cross section singularity of Sec.3.2 as we will show next.

### 3.4 Scattering Limit

The singularity of the Coulomb scattering cross section, for  $\theta_c \rightarrow 0$ , Eq.(3.15), becomes particularly apparent in the evaluation of the total Coulomb scattering cross section. That is, substitution of Eq.(3.15) into Eq.(3.4) gives

$$\sigma_s = 2\pi \int_{\theta_c=0}^{\pi} \left( \frac{K^2}{4 \sin^4(\theta_c/2)} \right) \sin(\theta_c) d\theta_c = \pi K^2 \int_{\theta_c=0}^{\pi} \frac{\cos(\theta_c/2)}{\sin^3(\theta_c/2)} d\theta_c. \quad (3.31)$$

To avoid the singularity as  $\theta_c \rightarrow 0$ , consider a finite non-zero lower bound  $\theta_{\min}$  and write

$$\begin{aligned} \sigma_s &= 2\pi K^2 \int_{\sin(\theta_{\min}/2)}^{\sin(\pi/2)} \frac{d[\sin(\theta)]}{\sin^3(\theta)}, \quad \theta = \frac{\theta_c}{2} \\ &= \pi K^2 \left\{ \left[ \sin\left(\frac{\theta_{\min}}{2}\right) \right]^{-2} - 1 \right\}. \end{aligned} \quad (3.32)$$

Note in this context that it is the collisions with small deflections which are responsible for the total Coulomb scattering cross section  $\sigma_s$  becoming very large.

A number of physical considerations suggest that  $\theta_{\min}$  should be chosen in accordance with a maximum impact parameter beyond which Coulomb scattering is relatively small. In a vacuum, the Coulomb field from a dominant isolated charge extends to infinity, implying therefore a scattering "deflection" interaction

at any arbitrary impact parameter. In a plasma, however, the target charge would be surrounded by a particle cloud of opposite charge. The fields due to surrounding particles will effectively "screen-out" the Coulomb field of an arbitrary charge at some maximum impact parameter distance which corresponds to some minimum scattering angle. This distance may be specified as the radius of an imaginary sphere surrounding a target ion such that the plasma electrons will reduce the target ion's Coulombic field by  $1/e$  at the sphere's surface. The Debye length,  $\lambda_D$ , as defined by Eq.(3.23a), evidently corresponds to this distance and we take the maximum impact parameter as

$$r_{o,max} = \lambda_D. \quad (3.33)$$

Thus,  $\theta_{min}$  follows from the inversion of Eq.(3.10):

$$\theta_{min} = 2 \tan^{-1} \left( \frac{K}{\lambda_D} \right). \quad (3.34)$$

Figure 3.5 displays the Coulomb scattering cross section for the case of d-t interactions and for comparison also shows the fusion cross section; as suggested previously, it is evident that Coulomb scattering events occur orders of magnitude more frequently than fusion reactions.

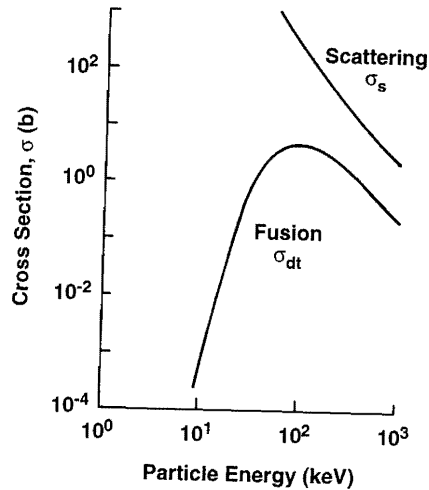


Fig. 3.5: Scattering cross section and fusion cross section for deuterium incident on a tritium target

### 3.5 Bremsstrahlung Radiation

An important consequence of scattering in fusion plasmas is bremsstrahlung radiation, which refers to the process of radiation emission when a charged particle accelerates or decelerates. It involves the transformation of some particle kinetic energy into radiation energy which—due to its relatively high frequency (X-ray wavelength range of  $\sim 10^{-9}$  m)—may readily escape from a plasma; thus, the kinetic energy of plasma particles is reduced, plasma cooling occurs, and a compensating energy supply may be required in order to maintain the desired plasma temperature.

A rigorous derivation of bremsstrahlung power emission in a hot plasma involves considerations of quantum mechanics and relativistic effects and is both tedious and time consuming. Indeed, even advanced methods of analysis require the imposition of simplifying assumptions if the formulation is to be at all tractable. It is, however, less difficult to develop an approximation of the dominant effect of the bremsstrahlung processes by the following considerations. A particle of charge  $q_e$  and moving with a time varying velocity  $v(t)$  will—according to classical electromagnetic theory in the nonrelativistic limit—emit radiation at a power

$$P \propto q_e^2 \left| \frac{dv}{dt} \right|^2. \quad (3.35)$$

In Fig. 3.6, we suggest this process for an electron moving in the electrostatic field of a heavy ion. To estimate the energy radiated per encounter, we replace  $|dv/dt|$  in Eq.(3.35) by an average acceleration  $\bar{a}$  to be calculated from Newton's Law,  $\bar{a} = \bar{F}_c / m$ , with  $\bar{F}_c$  representing the magnitude of the average Coulomb force approximated here by the electrostatic force between the two interacting particles when separated by the impact parameter  $r_o$ . That is, we take

$$\bar{a} \approx \frac{F_c(r_o)}{m} = \frac{Z q_e^2}{4\pi \epsilon_0 r_o^2 m} \quad (3.36)$$

for the average acceleration experienced by a particle of mass  $m$  and charge  $q_e$  in the field of a charge  $q_i = -Zq_e$ . Since an electron possesses a mass  $1/1836$  of that of a proton—with an even smaller ratio existing when compared to a deuteron or triton—the electrons in a plasma will therefore be the main contributors to bremsstrahlung radiation. We suggest this in Fig. 3.7 for a representative electron trajectory undergoing significant directional changes in a background of sluggish ions.

Imagining an electron ( $m_e, q_e$ ) to be in the vicinity of an ion ( $m_i, |q_i| = |Zq_e|$ ) for a time interval

$$\Delta t_o \approx \frac{r_o}{v_r} \quad (3.37)$$

with  $\bar{v}_r$  denoting the average relative speed between the electron and ion, we combine Eqs.(3.35) to (3.37) to assess the bremsstrahlung radiation energy per collision event as

$$\frac{E_{br}}{\text{collision}} \approx P \Delta t_o \propto \frac{Z^2 q_e^6}{m_e^2 r_o^3 \bar{v}_r}. \quad (3.38)$$

Note this expression refers to the collision of a single electron with an ion at the specific impact parameter  $r_o$ . Extending these considerations to a bulk of electrons of density  $N_e$  all approaching the ion with  $\bar{v}_r$ , then the number of electrons colliding per unit time with the same ion at the same impact parameter  $r_o$  is given by

$$\frac{dR_o}{\text{ion}} \approx N_e \bar{v}_r 2\pi r_o dr_o. \quad (3.39)$$

Multiplying this relation by the ion density  $N_i$  we obtain the differential electron-ion collision rate density

$$dR_o \approx N_e N_i \bar{v}_r 2\pi r_o dr_o \quad (3.40)$$

thereby accounting for all electron-ion interactions per unit volume and per unit time occurring about a specific impact parameter  $r_o$ .

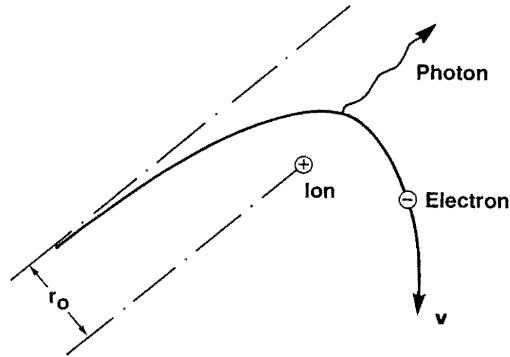


Fig. 3.6: Depiction of photon emission from an accelerated electron passing near an ion.

Next, in order to obtain the total bremsstrahlung radiation power density associated with the entire electron-ion force impact area, Eq. (3.38) needs to be multiplied by Eq.(3.40) and integrated over the range of the impact parameter  $r_{o,min}$  to  $r_{o,max}$ ; that is we now obtain for the bremsstrahlung power the proportionality

$$P_{br} \propto N_i N_e \frac{Z^2 q_e^6}{m_e^2} \int_{r_{o,min}}^{r_{o,max}} \frac{dr_o}{r_o^2}. \quad (3.41)$$

While  $r_{o,max} = \infty$  can be imposed, a finite minimum impact parameter needs to be specified due to the integral singularity for  $r_o \rightarrow 0$ . We choose to identify  $r_{o,min}$  with the DeBroglie wavelength of an electron, that is,

$$r_{o,min} = \frac{h}{m_e \bar{v}_e} \quad (3.42)$$

where  $h$  is Planck's constant and  $\bar{v}_e$  represents the average thermal electron speed defined by Eq.(2.19b):

$$\bar{v}_e = \sqrt{\frac{8kT_e}{m_e \pi}}. \quad (3.43)$$

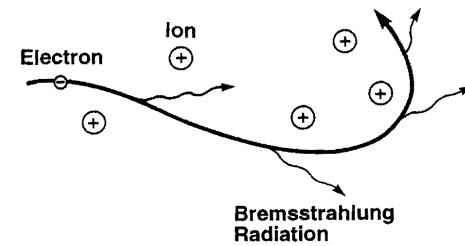


Fig. 3.7: Schematic depiction of an electron trajectory and bremsstrahlung radiation.

With the integration limits thus specified, the integral of Eq.(3.41) is readily evaluated so that the electron bremsstrahlung radiation power density is found to exhibit the following dominant dependencies:

$$P_{br} = A_{br} N_i N_e Z^2 \sqrt{kT} \quad (3.44)$$

where  $A_{br}$  is a constant of proportionality. For  $kT$  in units of eV and particle densities in units of  $m^{-3}$ ,

$$A_{br} \approx 1.6 \times 10^{-38} \left( \frac{m^3 J}{\sqrt{eVs}} \right) \quad (3.45)$$

which yields  $P_{br}$  in units of  $W \cdot m^{-3}$ . An important point to note here is that  $P_{br}$  is proportional to  $(kT)^{1/2}$ .

3.1 Examine the relationship between  $\theta_c$  and  $\theta_L$  for the limiting cases of  $m_b/m_a = \{0, 1, \infty\}$ .

3.2 For a typical case of d-t interaction at 5 keV, plot  $\sigma_s(\theta_c)$ ,  $0 \leq \theta_c \leq \pi$ .

3.3 For the conditions in problem 3.2, calculate  $\sigma_s$ , assuming a background particle density of  $10^{20} \text{ m}^{-3}$ .

3.4 Calculate the bremsstrahlung power increase if a d-t plasma were to contain totally stripped oxygen ions at a concentration of 1% of the electron density.

3.5 Calculate the ratio of bremsstrahlung power to fusion power for a d-t plasma with  $N_i = N_e = 10^{20} \text{ m}^{-3}$  at 2 keV and 20 keV.

3.6 Determine from a plot of power density versus kinetic temperature (use a double logarithmic scale) for a 50:50% D-T fusion plasma

(a) the so called ideal d-t ignition temperature  $T^*$ , i.e. the temperature at which the plasma fusion power density equals the loss power density due to bremsstrahlung.

(b) the temperature  $T_{ign}^*$  more relevant to fusion ignition since it refers to the plasma operational state where the bremsstrahlung loss power is balanced by the energy transfer from the fusion alphas to the background plasma per unit time by Coulomb collisions. Assuming that the charged particle fusion power is entirely transferred,  $T_{ign}^*$  is found from

$$f_{c,dt} P_{dt}(T_{ign}^*) = P_{br}(T_{ign}^*)$$

with  $f_{c,dt}$  representing the fraction of d-t fusion power allocated to charged particles (in this case  $\alpha$ 's). What does this condition mean for the overall power balance of the fusion plasma if other heat losses were neglected?

3.7 A fusion reactor using two opposing accelerators is proposed, where a 30 keV tritium beam from one is aimed head on at a 30 keV deuterium beam from the other. Would this work, and can you suggest improvements? What would you estimate is the maximum energy gain possible with this system (see Ch. 8)?

## PART II CONFINEMENT, TRANSPORT, BURN